separations

MDPI

Review

Separation Technologies for Iron and Aluminum Impurities in Rare Earth Solutions: Research Advancements and Prospects

Meng Zha [1,2], Xue Bian [1,2,*], Yinan Lv [1,2], Xuewen Mu [1,2], Yu Huang [1,2], Jing Wang [1,2] and Xinmiao Zhu [1,2]

[1] Key Laboratory of Ecological Metallurgy of Multi-Metal Intergrown Ores of Ministry of Education, Shenyang 110819, China
[2] School of Metallurgy, Northeastern University, Shenyang 110819, China
* Correspondence: bianx@smm.neu.edu.cn

Abstract

Rare earths are critical industrial raw materials with important strategic value. Impurity removal serves as the core step for rare earth separation and purification, as well as for improving product yield and quality. Compared with impurities such as silicon (Si), titanium (Ti) and vanadium (V), iron (Fe) and aluminum (Al) are widely associated with rare earth minerals and enter the feed solution at relatively high loads, making them the primary harmful impurities. During solvent extraction, Fe and Si-Al complexes readily cause emulsification and accumulate in the organic phase, which markedly deteriorates rare earth extraction performance. In precipitation processes, Fe and Al hydrolyze to form hydroxide colloids. These colloids tend to entrain rare earth species and induce resource loss. Driven by the rising purity requirements of rare earth products for advanced applications, conventional impurity removal technologies still suffer from insufficient selectivity and low treatment efficiency. This review summarizes the latest research advances in Fe and Al removal for rare earth feed solutions published since 2020, and systematically analyzes how Fe and Al impurities affect rare earth extraction and precipitation in different systems. The mechanisms and effects of additive introduction and electric field assistance in precipitation and extraction purification are discussed. Considering both impurity removal efficiency and cost, precipitation with electric-field enhancement is preferred for feedstocks containing high concentrations of Fe and Al, while solvent extraction or ion exchange is more suitable for low-level impurities. Emerging routes including supercritical extraction and ionic liquid dissolution remain at the laboratory scale; their industrial validation and operating costs are yet to be clarified.

Keywords: rare earths solution; Fe; Al; separation

Check for updates

Academic Editor: Hideo Maruyama

Received: 18 October 2026
Revised: 9 November 2026
Accepted: 12 November 2026
Published: 16 November 2026

Copyright: © 2026 by the authors. Licensee MDPI, Basel, Switzerland. This article is an open access article distributed under the terms and conditions of the Creative Commons Attribution (CC BY) license.

1. Introduction

Rare earth elements (REEs) are known as important industrial additives. Their importance in traditional metallurgy and high-end materials has become increasingly prominent. At present, only a few countries, including China, France, Australia, Malaysia, and Vietnam, can supply rare earth primary products such as rare earth carbonates, rare earth oxides, and rare earth metals on a large scale. This situation has accelerated research in many countries on industrial technologies for rare earth mineral smelting and secondary resource recovery. However, to extract rare earth products from rare earth ores or secondary resources, the technical challenges of REE separation and purification must be solved. In addition, rare earth applications impose strict requirements on the impurity content of rare earth primary products. Therefore, studying the sources and removal methods of impurities is critical [1].

Impurities such as Al and ferric iron (Fe(III)) pose significant challenges in REE processing flowsheets, especially in solvent extraction [2]. During the extraction of lanthanum (La) with P507 (2-ethylhexylphosphonic acid mono-2-ethylhexyl ester), a low concentration of Si in the organic phase exacerbates the emulsification caused by Al. The formation of microemulsions and rod-like polymers leads to emulsification during the extraction of Si-Al mixtures and pure Fe samples. In addition, the accumulation of impurities such as Si, Al, and Fe in the organic phase significantly reduces the extraction capacity for La [3]. Refractory metals such as Ti, V, and niobium (Nb) also readily hydrolyze to form fine particles. These particles are adsorbed by the solvent and thereby reduce the recovery of REEs [4]. Impurities in rare earth solutions markedly affect the recovery during precipitation. In the sulfuric acid treatment process of Bayan Obo rare earth concentrates, calcium (Ca) added during ore neutralization and pH adjustment precipitates as gypsum. REEs coprecipitate and lead to decreased recovery [5,6]. During rare earth carbonate precipitation, Al and Fe undergo hydrolysis to form colloidal hydroxides. This not only affects the formation of rare earth carbonates but also entrains REEs. Although Al, Fe, copper (Cu), and lead (Pb) do not affect the purity of rare earth precipitates during rare earth oxalate precipitation, these ions complex with oxalic acid and increase its consumption [1].

The removal of Fe and Al impurities is performed after REE leaching. In 2020, Judge, W. D. et al. [1] summarized and discussed methods for removing impurities from rare earth feed solutions. That article reviewed solvent extraction, ion exchange, precipitation, and other methods for removing impurities such as Fe and Al from rare earth feed solutions [1,7]. However, rare earth solution systems and the contents of Fe and Al impurities differ. The removal methods and their effects, therefore, differ markedly. For example, when solvent extraction is used with D2EHPA as the extractant in a phosphate system, Al is hardly co-extracted with REEs because hydrophilic $AlH_2PO_4^{2+}$ is formed. In a sulfate system, naphthenic acid is required as the extractant, and the O/A ratio and extractant concentration must be adjusted to remove Al ions from rare earth feed solutions. When ion exchange is used, an ethylenediamine acid ligand resin can serve as a cation-exchange material for the selective separation of REEs and Al. However, the exchange rate is low, and saturation requires 24 h. TEHDGA-impregnated resin can also selectively extract REEs from coal fly ash nitrate leach liquors and suppress the co-extraction of Fe and Al. Additionally, supercritical extraction and selective dissolution with ionic liquids are emerging methods for separating REEs from impurities in rare earth feed solutions. In the outlook on impurity removal methods, that article suggested that the structures of ion exchange resins, adsorbents, and solvent extractants must be understood in depth. Desorption behavior should be studied thoroughly. New extractants should be specially designed to improve selectivity for REEs.

In recent years, problems caused by impurities in rare earth feed solutions, such as extractant emulsification and product quality issues in industrial production, have remained prominent. This study analyzes the effects of Fe and Al impurities on extraction and precipitation in different rare earth solution systems. It also summarizes research progress on the removal of Fe and Al impurities from rare earth feed solutions since 2020. Finally, it provides an outlook on future research directions.

2. Effect of Iron and Aluminum Impurities in the Rare Earth Extraction Process

2.1. Effect of Iron Ions

When separating rare earth elements (REEs) using common acidic organophosphorus extractants such as D2EHPA (P204, HDEHP) and P507 (HEHEHP), REEs are extracted more readily than iron. Nevertheless, iron co-extraction still occurs at high Fe^{3+} concentrations in rare earth feed solutions [8–10]. D2EHPA is a dialkyl-phosphoric-acid-type extractant

with the textual structural formula $(2\text{-EH-O})_2P(=O)OH$. P507 belongs to the phosphonic acid monoester type, whose textual structural formula is 2-EH-P(=O)(OH)-O-2-EH. In non-polar diluents such as sulfonated kerosene, the two extractants form hydrogen-bonded dimers $H_2A_2 = [(2\text{-EH-O})_2P(=O)OH]_2$ and $H_2L_2 = [2\text{-EH-P}(=O)(OH)\text{-O-2-EH}]_2$, respectively. Cation-exchange extraction proceeds in low-acidity aqueous phases: dissociable protons from extractant dimers exchange with aqueous-phase metal ions, metal ions transfer into the organic phase, and H^+ is released to the aqueous phase.

The cation-exchange extraction reactions of RE^{3+}, Fe^{3+} and Al^{3+} in the D2EHPA system are shown in Equations (1)–(3):

$$RE^{3+}(aq) + 3H_2A_2(org) \rightleftharpoons RE[(2\text{-EH-O})_2P(=O)O]_3\cdot[(2\text{-EH-O})_2P(=O)OH]_3(org) + 3H^+(aq) \quad (1)$$

$$Fe^{3+}(aq) + 3[(2\text{-EH-O})_2P(=O)OH]_2(org) \rightleftharpoons Fe[(2\text{-EH-O})_2P(=O)O]_3\cdot[(2\text{-EH-O})_2P(=O)OH]_3(org) + 3H^+(aq) \quad (2)$$

$$Al^{3+}(aq) + 3[(2\text{-EH-O})_2P(=O)OH]_2(org) \rightleftharpoons Al[(2\text{-EH-O})_2P(=O)O]_3\cdot[(2\text{-EH-O})_2P(=O)OH]_3(org) + 3H^+(aq) \quad (3)$$

The corresponding extraction reactions for RE^{3+}, Fe^{3+} and Al^{3+} in the P507 system are given in Equations (4)–(6):

$$RE^{3+}(aq) + 3[2\text{-EH-P}(=O)(OH)\text{-O-2-EH}]_2(org) \rightleftharpoons RE\ [2\text{-EH-P}(=O)(O)\text{-O-2-EH}]_3\cdot[2\text{-EH-P}(=O)(OH)\text{-O-2-EH}]_3(org) + 3H^+(aq) \quad (4)$$

$$Fe^{3+}(aq) + 3[2\text{-EH-P}(=O)(OH)\text{-O-2-EH}]_2(org) \rightleftharpoons Fe\ [2\text{-EH-P}(=O)(O)\text{-O-2-EH}]_3\cdot[2\text{-EH-P}(=O)(OH)\text{-O-2-EH}]_3(org) + 3H^+(aq) \quad (5)$$

$$Al^{3+}(aq) + 3[2\text{-EH-P}(=O)(OH)\text{-O-2-EH}]_2(org) \rightleftharpoons Al\ [2\text{-EH-P}(=O)(O)\text{-O-2-EH}]_3\cdot[2\text{-EH-P}(=O)(OH)\text{-O-2-EH}]_3(org) + 3H^+(aq) \quad (6)$$

With increasing aqueous-phase acidity, the cation-exchange process is suppressed and extraction gradually shifts toward a solvating mechanism. After entering the P507-loaded organic phase, apart from forming the conventional extracted complex described by Equation (6), Al^{3+} can further coordinate with the P=O groups of P507 molecules to form stable P-O-Al-bridged complexes. These complexes are resistant to acid stripping and lead to continuous accumulation of aluminum impurities in the organic phase, as expressed by Equation (7):

$$Al^{3+}(aq) + 3[2\text{-EH-P}(=O)(OH)\text{-O-2-EH}]_2(org) \rightleftharpoons [Al(\text{-O-P}(=O)(2\text{-EH})\text{-O-2-EH})_3](org) + 3H^+(aq) \quad (7)$$

Our previous work investigated the chemical behavior of iron during P507 extraction in hydrochloric-acid media. Under appropriate pH conditions, Fe^{3+} undergoes hydrolysis and polymerization to form hydroxyl-iron polymers $Fe_x(OH)_y{}^{(3x-y)+}$, whose hydrolysis-polymerization equilibrium is presented in Equation (8). These polymers can assemble into long rod-like structures with lengths of tens of nanometers or more (Figure 1), and the degree of polymerization can reach up to 10^4. They are major triggers for extraction-system emulsification, inter-phase entrainment and poor phase-separation performance [3].

$$xFe^{3+}(aq) + yH_2O(l) \rightleftharpoons Fe_x(OH)_y{}^{(3x-y)+}(aq) + yH^+(aq) \quad (8)$$

In Equation (8), the values of x and y depend on solution pH, iron concentration and aging time. In sulfuric acid media, iron remains in the organic phase during REE extraction with D2EHPA [11]. By contrast, extremely low Fe co-extraction is observed for REE extraction using TODGA, Cyanex 923 and TBP in nitrate media [11,12]. Naphthenic acid is a carboxylic-acid-type cation-exchange extractant with the general formula R-COOH (where R represents alkyl groups containing saturated cyclopentyl or cyclohexyl moieties); metal separation is realized via proton exchange of carboxyl groups. For naphthenic-acid extraction, Fe^{3+} is extracted preferentially over REEs, yet iron gradually migrates toward the feed stage in counter-current extraction processes [13].

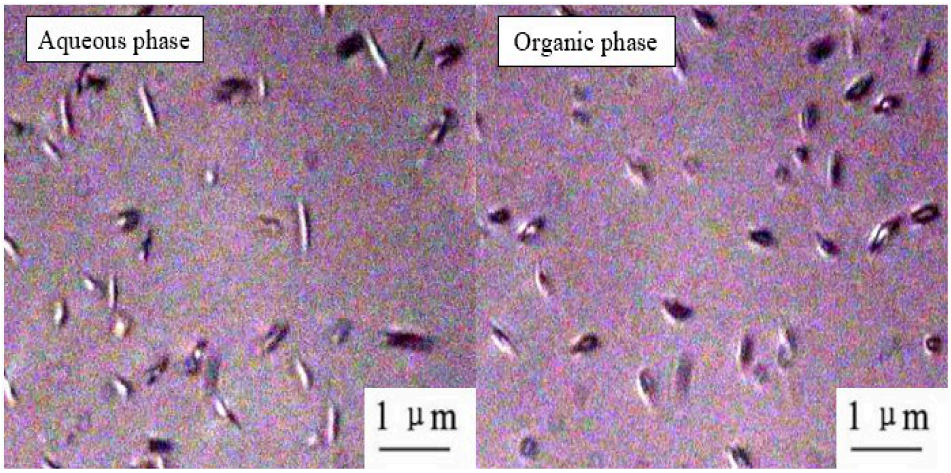


Figure 1. Polarization micro-images of aqueous and organic phases after extracting Fe. Saponification value of P507 = 0.4 mol/L; the concentrations of Fe = 12 g/L; O/A = 1; T = 25 °C.

In summary, during REE extraction with acidic extractants such as D2EHPA [8] or HEHEHP [10], appropriate control of the extractant concentration and O/A ratio can reduce the influence of Fe ions in solution. However, effective separation of REEs and Fe cannot be achieved. Reducing the extraction time can largely avoid the extraction of Fe(III) [14]. For example, when yttrium (Y) is extracted with D2EHPA and TBP, the extraction amount of Fe(III) is lowest when the extraction time is only 15 s [15].

2.2. Effect of Aluminum Ions

During REE solvent extraction, Al readily forms precipitates that cause emulsification of the extractant. Therefore, studying the effect of Al on REEs during solvent extraction is crucial.

In a hydrochloric acid system, acidic organophosphorus extractants such as D2EHPA and HEHEHP often extract some Al together with REEs, which reduces the purity of rare earth products [16]. In a phosphoric acid system, because hydrophilic $AlH_2PO_4^{2+}$ ions are formed, D2EHPA hardly extracts Al [8]. In a sulfuric acid system, when the O/A ratio and the concentrations of extractant and Al ions are high, Al ions are extracted together with REEs [9,10]. In the P507 system, Al (Figure 2c, Table 1 line 4) replaces H^+ in P-O-H and forms a P-O-Al structure. According to the above discussion, cation exchange is the main pathway for extracting Al or La from the aqueous phase with P507 (Figure 2d, Table 1 line 5). Because Al is present in the organic phase, the extraction capacity for La is significantly reduced. This indicates that Al is more readily extracted than La. The extraction capacity of the organic phase remains constant. Therefore, the accumulation of Al markedly reduces the extracted amount of La.

Table 1. Group absorption frequency.

Characteristic Peak	$v_{P=O}$ (cm^{-1})	$v_{P\text{-}O\text{-}C}$ (cm^{-1})	$v_{P\text{-}O\text{-}H}$ (cm^{-1})	$v_{O\text{-}P\text{-}O}$ (cm^{-1})
Saponated P507	1197.89	1039.32	975.61	866.82
Si	1197.62	1039.39	975.85	867.0
Si + Al	1185	1038	981	911.8
La	1163	1042	980.65	-

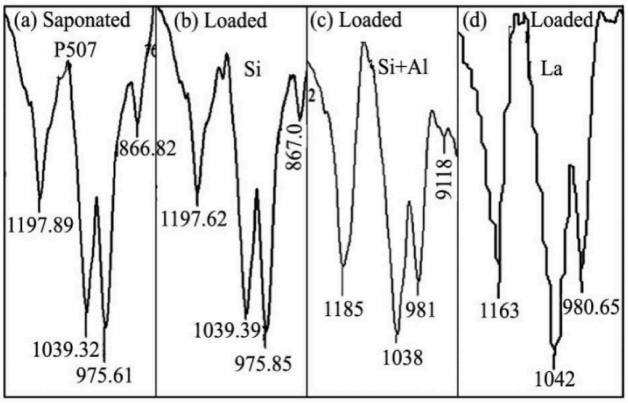


Figure 2. Enlarged view of bending vibration of P–O–H bond. Saponification value of P507 = 0.4 mol/L; the concentrations of Si and Al = 0.2 g/L; La concentration = 40 g/L; O/A = 1; T = 25 °C.

3. Methods for Removal of Iron and Aluminum Ions

3.1. Selective Leaching

Lei Zhang et al. [17] proposed a novel column leaching method using citric acid as the leaching solution, as shown in Figure 3. Under the action of hydrogen ions and citrate ions, REEs dissolve and are released from coal fly ash (CFA) particles. In the solution, rare earth cations formed rare earth–citrate complexes with citrate ions. These complexes were then carried away with the flowing liquid phase, which reduces their adsorption on the surface of CFA particles and thereby increases the leaching rate of REEs. Compared with the maximum recovery of total rare earth elements (TREEs) in traditional stirred leaching tests, which is less than 30%, the recovery of TREEs in the column leaching process increased to 64.8%. The leaching rates of impurities such as Al, Ti, and Fe are below 13.7%.

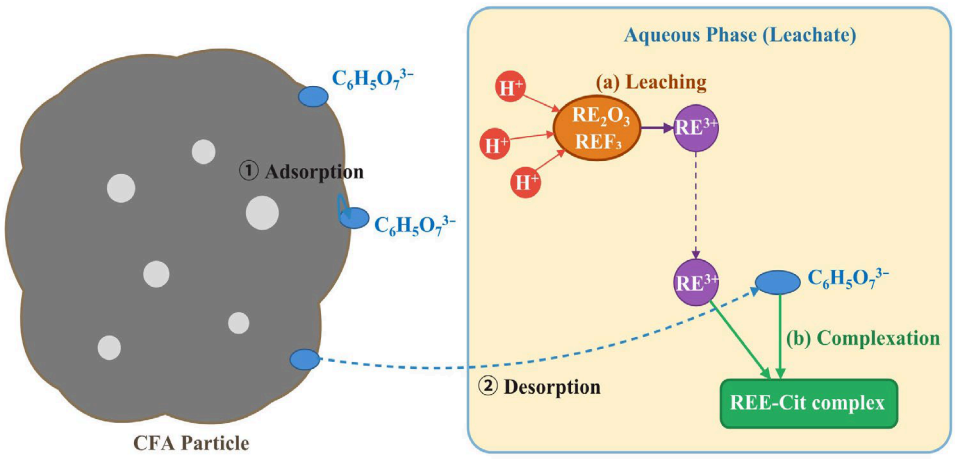


Figure 3. Conceptual diagram of the mechanism for column leaching to extract REEs from CFA.

Xin Chen et al. [18] introduced acetic acid (HAc) into the process of leaching REEs from ion-adsorption rare earth ores with magnesium (Mg) salts. REEs and HAc mainly exist in the form of $REAc_2^+$. This reduces the activation energy of the REE leaching reaction to 7.11 kJ/mol and increases the leaching rate. The HAc–Ac^- buffer system increases the pH value of the leaching process and promotes the hydrolysis of Al in the ion exchange phase. Meanwhile, DFT calculations [19] show that under the influence of acetate anions, it is difficult for Al^{3+} to adsorb onto the kaolinite (001) surface and form chemical bonds. This makes the adsorption of $(CH_3COO)_3Al$ the most difficult, thereby inhibiting the leaching of Al. As shown in Figure 4, under optimal conditions, the leaching rate of REEs reaches 98.40%,

while the leaching rate of Al is 66.61%. Compared with ammonium salt and magnesium salt leaching systems without acetic acid, the leaching rate of REEs was increased by more than 6%, while the leaching rate of Al was reduced by 23.33%.

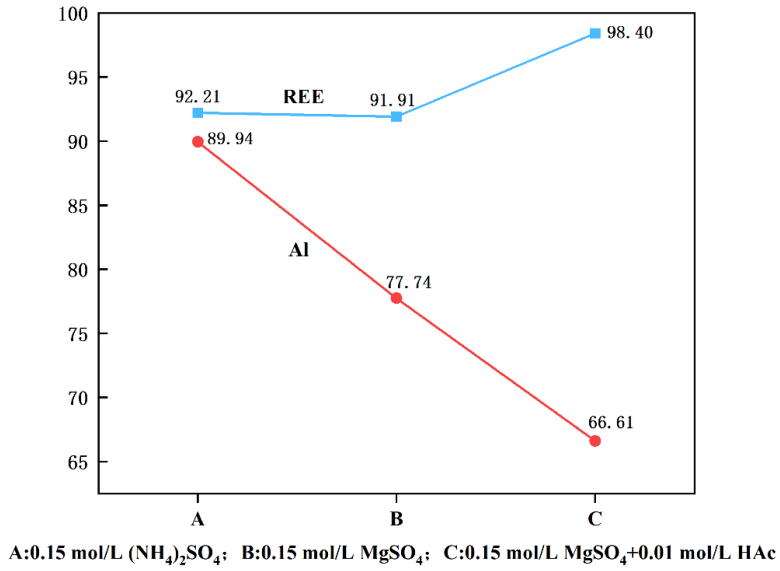


Figure 4. Effect of different leaching agents.

3.2. Solvent Extraction

Liqing Li et al. [20] used 8-hydroxyquinoline-modified silica gel (HQ-SiO_2) and 2,2′-(1,4-phenylenebis(oxy))dioctanoic acid (PPBOA) to construct an efficient impurity removal and rare earth enrichment process, as shown in Figure 5. Solid-phase extraction successfully removed 96.7% of the radioactive element thorium (Th). The aluminum concentration was reduced to 2.14 ppm by conventional chromatography. The REE concentration was enriched from 336.35 mg/L to 237.75 g/L by extraction-precipitation, which corresponds to an enrichment factor of more than 700. The rare earth content increased from 21.85% to 96.62%. The rare earth loss rate was controlled below 1.59%.

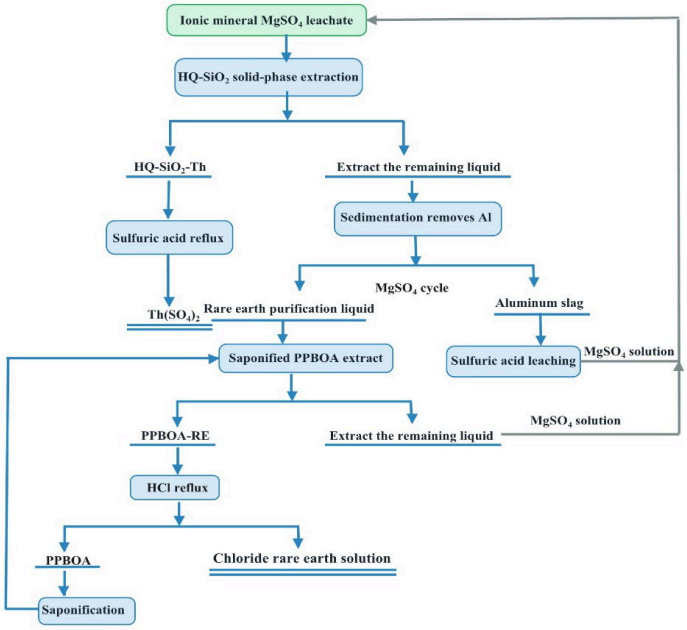
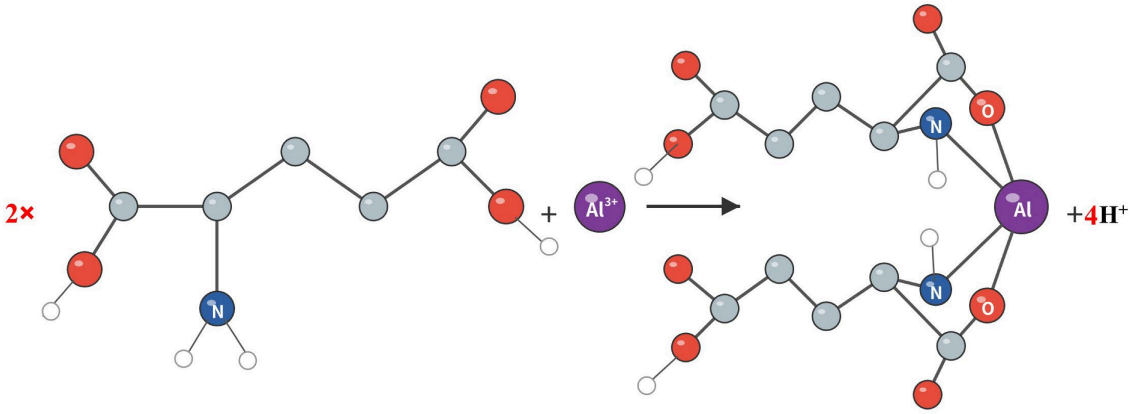


Figure 5. Flow chart of the proposed technological process.

Liang Gao et al. [21] employed Triton X-114 as the extractant and glutamic acid as the complexing agent for the selective extraction of Al ions. As shown in Figure 6, the amino and carboxyl groups of the amino acid form five-membered or six-membered ring structures with Al ions at a specific ratio, thereby increasing the extraction rate of Al. When the M_{glu}:M_{Al} ratio is 3:1, the solution pH is 4.5, the temperature is constant at 40 °C, and 10 mL of Triton X-114 is added after 10 min of reaction, the extraction rate of Al ions in a single extraction can reach 78.01%. The extraction rate of REEs after 10 min of equilibration is only 5.09%. This allows efficient separation of Al ions and rare earth ions in the mixed solution.



$$2H_2Glu + Al^{3+} \rightleftharpoons [Al(Glu)_2]^- + 4H^+$$

Figure 6. The reaction mechanism of glutamic acid with aluminum ions.

3.3. Precipitation

In solutions with low acidity and low Fe concentration, precipitation is very effective for Fe removal. However, as acidity increases, the operation of precipitation becomes complicated, and valuable metals are lost during the process [22]. For Al removal by precipitation, under strongly alkaline conditions, Al reacts with excess hydroxide ions to form water-soluble aluminate. Rare earth ions form hydroxide precipitates. Through sedimentation and filtration, rare earths are separated from the Al-containing solution [23].

Studies on the process parameter control of impurity removal from rare earth solutions using sodium (Na) hydroxide and ammonium bicarbonate precipitation show that pH is the key factor affecting impurity removal. The synergistic effect between temperature and concentration promotes the removal of impurities by sodium hydroxide and ammonium bicarbonate. The antagonistic effect between pH and temperature dominates the removal effect of the ammonium bicarbonate group. Under optimal conditions, the removal rates of Fe^{3+} and Al^{3+} by sodium hydroxide are about 100% and 64.9%, respectively. The removal rates of Fe^{3+} and Al^{3+} by ammonium bicarbonate are about 100% and 36.1%, respectively. However, when the precipitation pH exceeds 4, the loss rate of REEs increases sharply [24].

Yanzhu Liu et al. [25] proposed a precipitation method using a combination of ABC and triammonium citrate (TAC) to separate Al, La, and Ce. The pH ranges for Al and RE precipitation before and after TAC addition, calculated using Visual MINTEQ 3.1, are shown in Table 2. After adding a low concentration of TAC to the Al^{3+} solution, Al-citrate complexes are formed, which compete with the Al-hydroxide formation process. The coordination between TAC and Al^{3+} can reduce the pH value for Al^{3+} precipitation as $Al(OH)_3$ from 5.2 (Figure 7a) to 3.7 (Figure 7b). Therefore, in the pH range of 3.7 to 4.1, most Al^{3+} can be precipitated, while the loss of REEs is small. Studies also show that the optimal dosage of TAC has a linear relationship with the Al concentration or the molar ratio of Al to Fe. The optimal dosage of TAC is 4–5% of the Al content. After Al and Fe removal, a calcined rare earth oxide product

with a purity of 99.6% and an Al content of 0.31% can be obtained. Compared with processes without purification treatment or without TAC addition, the purity of rare earth oxides under this process is increased by 9.31% and 1.39%, respectively.

Table 2. Comparison table of precipitation pH values for different ions.

Ions	Without TAC		Add 1×10^{-4} mol/L TAC	
	Begin Precipitating the pH	Complete Precipitation of pH	Begin Precipitating the pH	Complete Precipitation of pH
Al^{3+}	2.4	5.2	2.0	3.7
La^{3+}	7.1	8.0	7.4	8.2

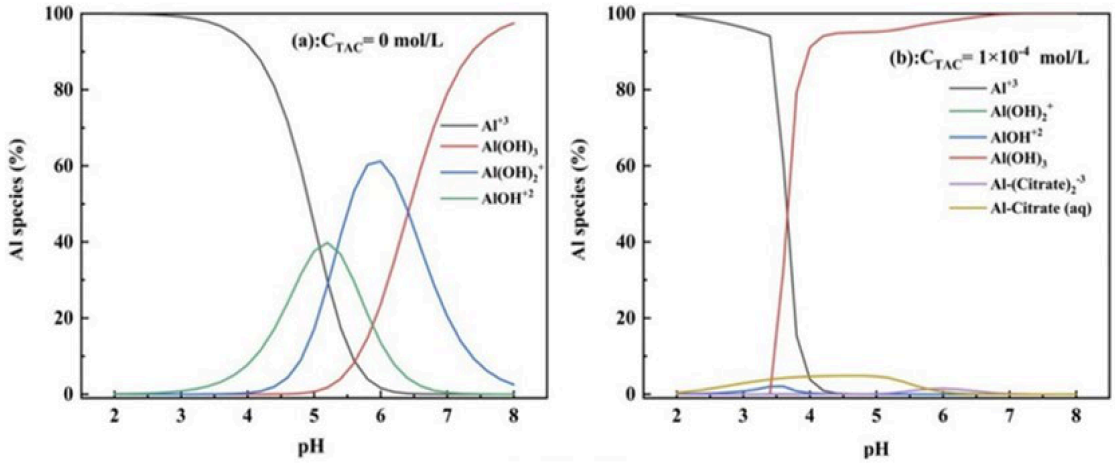


Figure 7. Effect of pH on the distribution (%) of aluminum species in $AlCl_3$ solution (0.007 mol/L) at 25 °C, in the presence of different TAC concentrations: (**a**) 0 mol/L, (**b**) b:1×10^{-4}mol/L.

The acid method for Al removal is suitable for rare earth-rich solutions with low Al content. Studies have found that in an acidic environment, oxalic acid first reacts with Al ions to form an aluminum oxalate precipitate. When oxalic acid is in excess, the aluminum oxalate precipitate dissolves in oxalic acid, while the rare earth oxalate precipitate has low solubility. Based on the difference in solubility between aluminum oxalate and rare earth oxalate in acidic solution, Al removal is achieved [26].

Lauryl glucoside (LG) was used by Xianping Luo et al. [27] as a precipitant to remove impurities from ion-adsorption rare earth leaching solutions. The experimental results shown in Figures 8 and 9 and Table 3 indicate that LG reacts with impurity metal ions to form new Al-O chemical bonds. This makes the adsorption energy between LG and $Al(OH)_3$ significantly higher than that between LG and $RE(OH)_3$. Therefore, the removal rate of Al^{3+} in the leaching solution can reach 99.09 ± 1.9%, the removal rate of Fe^{3+} can reach 93.13 ± 1.3%, and the rare earth loss rate is only 5.33 ± 0.9%. When NH_4HCO_3 is used as the precipitant and the leaching solution pH is 5.4, the removal rates of Al^{3+} and Fe^{3+} are 91.03 ± 0.1% and 92.53 ± 0.2%, respectively, while the rare earth loss rate reaches 23.27 ± 1.3%.

Huaping Nie et al. [28] studied a lanthanum chloride feed solution and used ammonium bicarbonate as the precipitant. They investigated the effects of complexing agent type, temperature, complexing agent dosage, precipitant dosage, and reaction time on the purification of a lanthanum chloride feed solution in an ammonium bicarbonate system. The results show that salicylic acid has the best complexing effect. In the ammonium bicarbonate system, the optimal process conditions are a temperature of 35 °C, a salicylic acid

dosage of 2.5 times the theoretical amount, a precipitant dosage of 1.75 times the theoretical amount, and a reaction time of 2.5 h. Under these conditions, after the reaction of the feed solution, the precipitation rate of Fe^{3+} is only 0.42%, the precipitation rate of Al^{3+} is 10.51%, and the precipitation rate of La^{3+} reaches 99.99%. The purity of the final lanthanum oxide powder product reaches 99.99%.

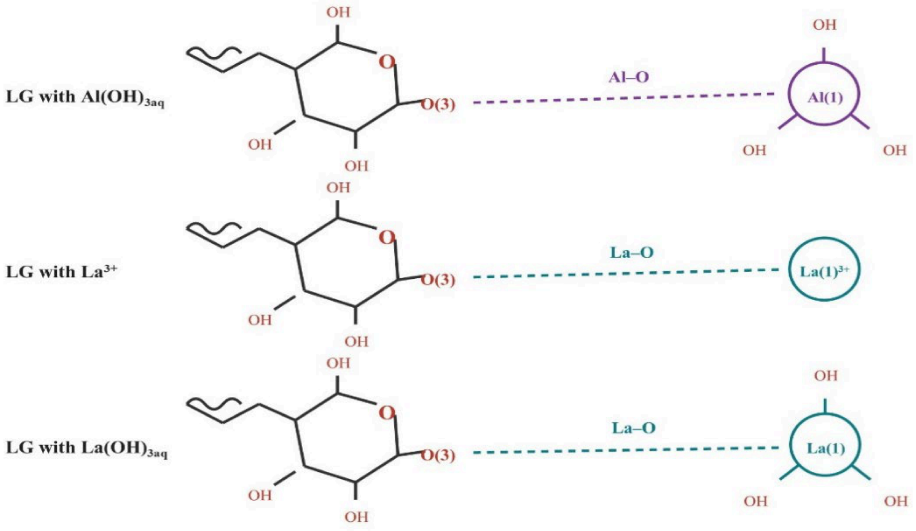


Figure 8. Ideal model of the reaction products of LG with $Al(OH)_3$, La^{3+} and $La(OH)_3$.

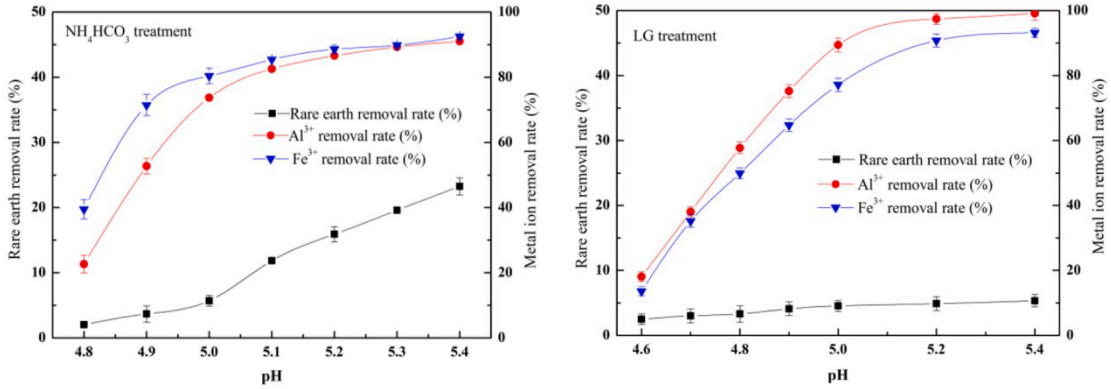


Figure 9. Metal ion removal rate at different pH values adjusted with NH_4HCO_3 and LG.

Table 3. Adsorption energy of ions interacting with LG and the bond population of reagent reaction by MS.

Compound Composition	LG + $Al(OH)_3$	LG + La^{3+}	LG + $La(OH)_3$
Adsorption energy ($KJ \cdot mol^{-1}$)	−114.82	−45.94	−70.58
Reaction bond	Al_1-O_3	La_1-O_3	La_1-O_3
Bond population	0.26	0.01	0.10
Bond length (Å)	1.95742	2.83316	2.57417

A process for the selective precipitation of Al, Fe, and Th from pregnant leach solution (PLS) containing REEs using magnesium carbonate as the precipitant was investigated by Sicheng Li et al. [29] through aqueous thermodynamic modeling and kinetic experiments. At pH 3.6, H_2O_2 addition is 0.52 mL, Fe is almost completely removed, the removal rate of Al is about 65%, and the total loss rate of REEs is less than 3%. A techno-economic analysis for a PLS treatment plant with a daily processing capacity of 1000 m^3 in Ontario, Canada,

shows that the monthly operating cost is about 2.65 million USD, and the capital cost is about 7.85 million USD.

Di Wu et al. [30] took advantage of the strong adsorption capacity of aluminum-based supports for impurity precipitates in rare earth solutions. Lanthanum-cerium oxide (LCO) was added to adjust the pH of the initial rare earth solution from 1.12 to 4.0, so that impurity hydroxides precipitated and were adsorbed onto the surface of the aluminum-based support. Under the conditions of an aluminum-based support dosage of 20 g/100 mL and a water bath temperature of 30 °C, the removal efficiencies of Al^{3+} and Fe^{3+} reached 97.5% and 92.7%, respectively. The solid generated after purification can be converted into regenerated aluminum-based supports for reuse after washing, drying and calcination. After three cycles, the variation in removal rates of non-rare earth anions and cations was less than 3%. This process opens up a new application scenario for abundant lanthanum and cerium, and avoids the risk of introducing new impurities from conventional alkaline sources.

3.4. Other Methods

Electrochemical methods were adopted to remove impurities from rare earth feed solutions. The basic principle lies in the pH difference for hydroxide precipitation between impurities such as Fe and Al and rare earth elements (REs). An applied electric field can raise the pH near the cathode (reaction shown below), thus realizing the preferential precipitation of impurities.

Yaoyao Zhu et al. [31] regulated the generation rate of hydroxide ions via electrochemistry. A large amount of hydroxide ions was produced during electrolysis to elevate solution pH. Taking advantage of the difference in precipitation pH between aluminum and rare earth elements, aluminum was removed from the rare earth solution. Under optimized conditions, the aluminum removal rate reached 88.35%, while the rare earth loss was only 5.99%. For comparison, ammonium bicarbonate precipitation yielded an aluminum removal rate of 85.04%, but the rare earth loss rose to 11.15%.

$$O_2 + 2H_2O + 4e \rightarrow 4OH^- \quad (9)$$

$$2H_2O + 2e \rightarrow 2OH^- + H_2 \uparrow \quad (10)$$

To suppress the diffusion of RE^{3+} and the neutralization between H^+ and OH^- during aluminum removal via the electrochemical method, Dongyue Xie et al. [32] proposed an approach combining anion membrane electrolysis (AME) with cyclone electrolysis. Compared with mechanical mixing, cyclone mixing reduces rare earth loss and improves aluminum removal efficiency. Under optimum conditions, the aluminum removal rate reaches 93.3%, with a rare earth loss rate of only 1.84%. The rare earth loss is attributed to the locally elevated pH near the cathode, which leads to the direct deposition of $RE(OH)_3$ on the electrode surface. Chenjiahui Wang et al. [33] adopted nickel foam as the cathode in the electrochemical aluminum removal process. This configuration effectively lowers the current density and restrains the formation of strongly alkaline local regions, maintaining the pH near the cathode below the precipitation threshold of rare earth elements. The inhibition of rare earth hydrolysis on the nickel foam cathode surface enables the in situ generated hydroxides during electrolysis to diffuse more efficiently into the bulk solution. Consequently, an aluminum removal rate of 94.26% and a rare earth loss rate of 4.95% are achieved.

Zhiyuan Zeng et al. [34] developed a bis(2-ethylhexyl)glycinate ionic liquid ([DOC4mim][DEHG]) for removing Al impurities from ion-adsorption rare earth ore leaching solutions. In a sulfuric acid system, this ionic liquid extracts Al through an ion-association mechanism. When the concentration of [DOC4mim][DEHG] is 40–42.5 mmol/L,

the initial pH of the aqueous phase is 4, and 0.5 mol/L sodium sulfate is added to the aqueous phase, the removal rate of Al in the leaching solution exceeds 95%, and the recovery rate of REEs also exceeds 96%. This study provides new insights into the efficient and sustainable removal of Al impurities from actual rare earth leaching solutions.

Nian Zhang et al. [35] synthesized methyltrioctylammonium chloride ([N1888]Cl) and industrial naphthenic acid (NA) for the purification of Al^{3+} from $GdCl_3$ solution. Under the experimental conditions, the extraction properties of diluted [N1888][NA], diluted NA and saponified NA were comparatively investigated and the separation factors of Al/Gd were 23.0 in diluted [N1888][NA] system. The removal efficiency of Al^{3+} was 99.4%, and the purity of Gd^{3+} was 99.998%.

Coal gangue was calcined at 600 °C by Jingzheng Wang et al. [36]. Then 5% ferric sulfate was added, and mechanochemical activation treatment was performed. This process changes the surface and crystal structure of coal gangue, promoting the release of rare earth phosphate minerals and the formation of rare earth sulfates. At the same time, ferric sulfate is converted into insoluble iron oxide, which fixes impurities and promotes selective leaching of REEs. During the leaching process, the rare earth leaching rate exceeds 65%, while the leaching rates of Al and Fe are only 0.37% and 1.27%, respectively.

4. Conclusions and Outlook

As the main raw materials for rare earth extraction, Bayan Obo rare earth concentrates, bastnaesite, and monazite concentrates all contain impurities such as Fe and Al, as shown in Table 4 [37–39]. Fe and Al impurities in rare earth feed solutions cause extraction emulsification and the entrainment of rare earths during coprecipitation, reducing product purity and rare earth recovery. As shown in Table 5, different impurity removal methods differ significantly in process conditions, impurity removal effects, production costs, and industrial adaptability. Selective leaching uses combinations of inorganic and organic acids, such as citric acid column leaching and magnesium salt-acetic acid composite systems. By utilizing the differences in stability constants of RE, Fe, Al, and organic complexing agents as shown in Table 6 [40–44], Fe and Al can be preliminarily separated from REEs in the leaching step. The process is simple, and the cost of organic acids is moderate. However, the separation efficiency of impurities from REEs is relatively low, so it can be used as a pretreatment method. Solvent extraction has high separation efficiency, and ionic liquids are more efficient for removing Fe and Al. However, most extraction systems are sensitive to pH, phase ratio, and temperature. At the same time, ionic liquids and modified silica gel have relatively high costs, and some systems are prone to emulsification. This method is suitable for deep impurity removal from medium- and high-concentration rare earth feed solutions. Precipitation is the mainstream industrial method, with simple operation and low equipment investment. Alkali precipitation and ammonium bicarbonate precipitation can almost completely remove Fe. However, when pH exceeds 4, rare earth loss increases sharply.

Table 4. Content of rare earth elements, Fe, and Al in major rare earth minerals.

Composition (wt.%)	REO	T_{Fe}	Al_2O_3	References
Mixed rare earth concentrate	59.05	2.77	0.074	[37]
Bastnaesite concentrate	72.14	0.84	0.1	[38]
Monazite	58.34	<0.01	<0.01	[39]

Table 5. Comparison of methods for removing Fe and Al from rare earth solution.

	Removal Mechanism	Parameters	Separation Efficiency	Advantage	Disadvantage	References
Source reduction	Selective leaching	Citric acid conditions = 1 mol/L	The leaching rates of TREEs, Al, and Fe were 64.8%, 7.2%, and 13.7%.	Reduced the amount of Fe and Al entering the rare earth solution, thereby alleviating the pressure associated with impurity removal from the rare earth solution.	The removal efficiency is poor, which could readily lead to rare earth losses during leaching.	[17]
		Flow rate = 0.4 mL/min				
		$MgSO_4$ concentration = 0.15 mol/L	The leaching efficiencies of TREEs and Al were 98.40% and 66.61%.			[18]
		HAc concentration = 0.01 mol/L				
		pH = 5.50				
		Liquid–solid ratio = 1.5				
		Flow rate = 0.6 mL/min				
Aftertreatment	Solvent extraction	Triton X-114	The extraction rates of TREEs and Al were 26% and 78.01%.	The process could operate continuously.	The separation factor for rare earth elements and impurities still required further improvement.	[21]
		Mglu:Mal = 3:1				
		pH = 4.5				
		Temperature of 40 °C				
		Time = 10 min				
		8-hydroxyquinoline modified silica gel (HQ-SiO_2)	Adsorption efficiencies were 79.9% for Al, and 13.1% for RE respectively.			[20]
		pH = 4.03				

Table 5. *Cont.*

	Removal Mechanism	Parameters	Separation Efficiency	Advantage	Disadvantage	References
Aftertreatment	Precipitation	NaOH concentrations = 4 mol/L	The removal rates of Fe^{3+}, $A1^{3+}$ and REE recovery by NaOH were about 100%, 64.9% and 99.7%.	The process was well-established and demonstrates superior performance in removing high-concentration impurities.	Added additives could readily lead to pollution from organic-containing wastewater and pose a high-cost risk.	[24]
		pH = 4				
		Temperature = 50.0 °C				
		NH_4HCO_3 concentrations = 1.5 mol/L	The removal rates of Fe^{3+}, $A1^{3+}$ and REE recovery were about 100% 36.1% and 94.4%.			[24]
		pH = 4				
		Temperature = 40 °C				
		pH = 3.7–4.1	The removal efficiency of iron, aluminum and the loss of REs during precipitation are 100%, 93% and 5.6%			[25]
		TAC is 4–5% of the aluminum content				
		pH = 5.4	The removal rates of Al^{3+}, Fe^{3+} and rare earth loss rate were 99.09 ± 1.9%, 93.13 ± 1.3% and 5.33 ± 0.9%.			[27]
		Lauryl glucoside (LG) = 0.1 mol·L^{-1}				
		Temperature = 35 °C	Precipitation rates of Fe^{3+}, Al^{3+}, and La^{3+} were 0.42%, 10.51%, and 99.99%.			[28]
		Salicylic acid = 2.5 times the theoretical amount				
		Ammonium bicarbonate = 1.75 times the theoretical amount				
		Reaction time = 2.5 h.				

Table 5. *Cont.*

	Removal Mechanism	Parameters	Separation Efficiency	Advantage	Disadvantage	References
Aftertreatment	Precipitation	$MgCO_3$ concentrations = 20 wt%	Enabled complete removal of iron The removal efficiency of aluminum was 65%, and TREE losses under 3%.	The process was well-established and demonstrates superior performance in removing high-concentration impurities.	Added additives could readily lead to pollution from organic-containing wastewater and pose a high-cost risk.	[29]
		Temperature = 81 °C				
		pH = 3.6				
		H_2O_2 addition = 0.52 mL				
		Equilibrium time = 30 min				
	Electrochemical assistance	Lanthanum–cerium oxides to adjust the pH Aluminum-based carrier adsorbed hydroxide precipitation of impurities pH = 4.0 Temperature = 25 °C	The removal efficiencies of Al^{3+}, Fe^{3+} were 97.5% and 92.7%. The rare earth average loss rate was under 2%.			[30]
		Temperature = 25 °C, Current density = 100 A/m^2, pH = 3.90	The removal efficiency of aluminum was 88.35% and TREE losses were 5.99%.	Based on the principle of sedimentation and impurity removal, an electric field was introduced to improve the sedimentation efficiency of impurities.	These methods were still in the laboratory research stage; the design of the equipment for large-scale application and its power consumption costs required further investigation.	[31]
		Anion-exchange membrane electrolysis (AME) combined with cyclone electrolysis Rotational speed = 300 rpm pH = 4.9~5.0, Kinetic effect of hydroxide ion generation and transfer Current density = 0.67 mA/cm^{-2}	The removal efficiency of aluminum was 93.3%, and TREE losses were 1.84%.			[32]
		3D cathode Current density = 0.3 mA/cm^2 Stirring speed = 400 rpm pore density = 130 PPI	The removal efficiency of aluminum was 94.26%, and TREE losses were 4.95%.			[33]

Table 5. *Cont.*

	Removal Mechanism	Parameters	Separation Efficiency	Advantage	Disadvantage	References
Aftertreatment	Ionic liquid extraction	[DOC4mim][DEHG] concentration = 40–42.5 mmol/L	The removal rates of $A1^{3+}$ and REE recovery were above 95% and 96%	The separation of impurities from rare earths is highly effective, and the ionic liquids offer significant environmental advantages.	The cost of large-scale production of ionic liquids still needs to be reduced.	[34]
		pH = 4				
		Na_2SO_4 concentration = 0.5 mol/L				
		$C_{[N1888][NA]}$ = 0.1 mol/L	$\beta_{Al/Gd}$ = 23.0			[35]
		pH = 1.0–3.0	The removal efficiency of Al^{3+} was 99.4%, and the purity of Gd^{3+} was 99.998%.			
		NaCl concentration = 0.6 mol/L				
	Solid-phase transformation	Calcination temperature = 600 °C	The leaching rates of aluminum (Al) and iron (Fe) were only 0.37% and 1.27%, with a leaching efficiency of 65% for REEs.	To prevent the leaching of impurities; the approach was the opposite of that used for impurity removal from rare earth solutions.	To prevent the leaching of impurities, the rare earth leaching rate was relatively low.	[36]
		$Fe_2(SO_4)_3$ addition = 5%				
		Mechanical–chemical activation time = 1 h				

Note: Economic-cost data are not included in this table.

Table 6. Complexation stability constants of rare earth elements, Fe, and Al with citric acid [40–44].

Elements	Complex Formation Reaction	$\log K_1$ (25 °C)
Fe^{3+}	$Fe^{3+} + Cit^{3-} \leftrightharpoons FeCit$	13.3
Al^{3+}	$Al^{3+} + Cit^{3-} \leftrightharpoons AlCit$	7.37
Ce^{3+}	$Ce^{3+} + Cit^{3-} \leftrightharpoons CeCit$	6.95
La^{3+}	$La^{3+} + Cit^{3-} \leftrightharpoons LaCit$	6.75

Overall, in industry, precipitation is usually the preferred method for high concentrations of Fe and Al impurities, while solvent extraction or ion exchange is employed for further removal of low-concentration impurities. Traditional precipitation has the lowest overall cost and is suitable for large-scale production. Solvent extraction and ionic liquids have excellent impurity removal effects but relatively high costs. Selective leaching is suitable for source reduction in impurities. Therefore, a combined process of selective leaching pretreatment, preliminary impurity removal by precipitation, and deep purification by solvent extraction can be adopted to balance impurity removal effects and economic benefits.

Author Contributions: M.Z.: Investigation, Formal analysis, Writing—original draft. X.B.: Conceptualization, Supervision, Writing—review & editing, Project administration. Y.L.: Investigation, Visualization, Writing—original draft. X.M.: Resources, Validation. Y.H.: Resources, Validation. J.W.: Investigation, Formal analysis. X.Z.: Resources, Validation. All authors have read and agreed to the published version of the manuscript.

Funding: This research was funded by the National Science and Technology Major Project of Deep Earth grant number 2026ZD1014003.

Data Availability Statement: No new data were created or analyzed in this study. Data sharing is not applicable to this article.

Conflicts of Interest: The authors declare no conflict of interest.

References

1. Judge, W.D.; Azimi, G. Recent progress in impurity removal during rare Earth element processing: A review. *Hydrometallurgy* **2020**, *196*, 105435. [CrossRef]
2. Battsengel, A.; Batnasan, A.; Narankhuu, A.; Haga, K.; Watanabe, Y.; Shibayama, A. Recovery of light and heavy rare earth elements from apatite ore using sulphuric acid leaching, solvent extraction and precipitation. *Hydrometallurgy* **2018**, *179*, 100–109. [CrossRef]
3. Wu, W.; Zhang, F.; Bian, X.; Xue, S.; Yin, S.; Zheng, Q. Effect of loaded organic phase containing mixtures of silicon and aluminum, single iron on extraction of lanthanum in saponification P507-HCl system. *J. Rare Earths* **2013**, *31*, 722–726. [CrossRef]
4. Ritcey, G.M. Crud in solvent extraction processing-a review of causes and treatment. *Hydrometallurgy* **1980**, *5*, 97–107. [CrossRef]
5. Dutrizac, J.E. The behaviour of the rare Earth elements during gypsum ($CaSO_4 \cdot 2H_2O$) precipitation. *Hydrometallurgy* **2017**, *174*, 38–46. [CrossRef]
6. Azimi, G.; Papangelakis, V.G.; Dutrizac, J.E. Modelling of calcium sulphate solubility in concentrated multi-component sulphate solutions. *Fluid Phase Equilib.* **2007**, *260*, 300–315. [CrossRef]
7. Zhang, Z.; Jia, Q.; Liao, W. Chapter 277-Progress in the Separation Processes for Rare Earth Resources. In *Including Actinides, Handbook on the Physics and Chemistry of Rare Earths*; Elsevier: Amsterdam, The Netherlands, 2015; Volume 48, pp. 287–376. [CrossRef]
8. Ye, Q.; Li, G.; Deng, B.; Luo, J.; Rao, M.; Peng, Z.; Zhang, Y.; Jiang, T. Solvent extraction behavior of metal ions and selective separation Sc^{3+} in phosphoric acid medium using P204. *Sep. Purif. Technol.* **2019**, *209*, 175–181. [CrossRef]
9. Shi, W.; Li, J.; Liu, S.; Zhou, L.; Lai, Y.; Zhu, Y.; Zhang, H.; Qi, T. Efficient separation and comprehensive recovery of rare earth, bismuth and iron by one-step extraction and two-step stripping. *J. Ind. Eng. Chem.* **2025**, *141*, 145–153. [CrossRef]
10. Huang, X.; Dong, J.; Wang, L.; Feng, Z.; Xue, Q.; Meng, X. Selective recovery of rare earth elements from ion-adsorption rare earth element ores by stepwise extraction with HEH (EHP) and HDEHP. *Green Chem.* **2017**, *19*, 1345–1352. [CrossRef]
11. Kim, D.; Powell, L.E.; Delmau, L.H.; Peterson, E.S.; Herchenroeder, J.; Bhave, R.R. Selective extraction of rare earth elements from permanent magnet scraps with membrane solvent extraction. *Environ. Sci. Technol.* **2015**, *49*, 9452–9459. [CrossRef] [PubMed]

12. Gergoric, M.; Ekberg, C.; Foreman Mark, R.S.T.J.; Steenari, B.; Etegan, T. Characterization and leaching of neodymium magnet waste and solvent extraction of the rare-earth elements using TODGA. *J. Sustain. Metall.* **2017**, *3*, 638–645. [CrossRef]
13. Balinski, A.; Kelly, N.; Helbig, T.; Meskers, C.; Reuter, M.A. Separation of Aluminum and Iron from Lanthanum—A Comparative Study of Solvent Extraction and Hydrolysis-Precipitation. *Minerals* **2020**, *10*, 556. [CrossRef]
14. Zhang, G.; Chen, D.; Wei, G.; Zhao, H.; Wang, L.; Qi, T.; Meng, F.; Meng, L. Extraction of iron (III) from chloride leaching liquor with high acidity using tri-n-butyl phosphate and synergistic extraction combined with methyl isobutyl ketone. *Sep. Purif. Technol.* **2015**, *150*, 132–138. [CrossRef]
15. Goode, J.R. Thorium and rare earth recovery in Canada: The first 30 years. *Can. Metall. Q.* **2013**, *52*, 234–242. [CrossRef]
16. Zhao, Z.; Qiu, Z.; Yang, J.; Lu, S.; Cao, L.; Zhang, W.; Xu, Y. Recovery of rare earth elements from spent fluid catalytic cracking catalysts using leaching and solvent extraction techniques. *Hydrometallurgy* **2017**, *167*, 183–188. [CrossRef]
17. Zhang, L.; Chen, H.; Pan, J.; Yang, F.; Long, X.; Yang, Y.; Zhou, C. Rare earth elements recovery and mechanisms from coal fly ash by column leaching using citric acid. *Sep. Purif. Technol.* **2025**, *353*, 128471. [CrossRef]
18. Chen, X.; Chen, J.-F.; Li, J.-Q.; Li, H.; Xu, J.-F.; Xiao, Y.-F. Strengthening rare earth and inhibiting aluminum leaching in magnesium salt-acetic acid compound system from ion-adsorption type rare earth ore. *Sep. Purif. Technol.* **2024**, *334*, 126070. [CrossRef]
19. Long, Q.; Yan, H.; Wu, H.; Qiu, S.; Zhou, X.; Qiu, T. Influence mechanism of leaching agent anions on the leaching of aluminium impurities in ionic-type rare earth ores: A DFT simulation combined with experimental verification. *Sep. Purif. Technol.* **2025**, *354*, 128768. [CrossRef]
20. Li, L.; Liu, C.; Zhang, H.; Huang, B.; Luo, B.; Bie, C.; Sun, X. The enrichment of rare earth from magnesium salt leaching solution of ion-adsorbed type deposit: A waste-free process for removing impurities. *J. Environ. Manag.* **2022**, *310*, 114743. [CrossRef] [PubMed]
21. Gao, L.; Wang, Y.; Oyang, J.; Gao, Y.; Liu, J.; Wang, R.; Xu, Z.; Li, J. Removal of Aluminum from Synthetic Rare Earth Leach Solution by Selective Complexation and Turbidity Point Extraction. *Minerals* **2023**, *13*, 1462. [CrossRef]
22. Chang, Y.; Zhai, X.; Li, B.; Fu, Y. Removal of iron from acidic leach liquor of lateritic nickel ore by goethite precipitate. *Hydrometallurgy* **2009**, *101*, 84–87. [CrossRef]
23. Zhang, L.; Gao, J.; Damoah, L.N.W.; Robertson, D.G. Removal of Iron From Aluminum: A Review. *Mineral. Process. Extr. Metall. Rev.* **2012**, *33*, 99–157. [CrossRef]
24. Wu, Y.; Zhang, S.; Wang, G.; Li, T.; Xu, X.; Pu, Y.; Zhou, W.; Li, Y.; Jia, Y. Impurity removal of acid leachates from rare earth slag with sodium hydroxide and ammonium bicarbonate: Mechanism and efficiency optimization. *J. Clean. Prod.* **2023**, *423*, 138782. [CrossRef]
25. Liu, Y.; Nie, F.; Liu, L.; Ding, Y.; Ma, Y.; Ding, Z.; Zhao, Q.; Li, Y. Efficient separation of Al and Fe impurities from La-Ce chloride solution by pH adjustments with ammonium bicarbonate in the presence of triammonium citrate. *Hydrometallurgy* **2025**, *238*, 106578. [CrossRef]
26. Wu, X.; Wang, Z.; Xia, C.; Shi, X.; Luo, T.; Bao, X.; Liu, R.; Xie, S. Kinetics study on leaching of rare earth and aluminum from polishing powderwaste using hydrochloric acid. *J. Rare Earths* **2020**, *38*, 1009–1018. [CrossRef]
27. Luo, X.; He, K.; Zhou, H.; Zhang, Y.; Xie, F. Enhanced impurity removal of ionic rare earth leaching solution through the use of lauryl glucoside. *Miner. Eng.* **2022**, *181*, 107551. [CrossRef]
28. Nie, H.; Xiao, W.; Wang, J.; Zhang, Z. Behavior rule of iron and aluminum elements in course of impurity removal coordinated with lanthanum chloride feed solution. *Chin. J. Nonferrous Met.* **2024**, *34*, 4159−4169.
29. Li, S.; Sauber, M.E.; Sun, T.; Azimi, G. Iron, aluminum, and thorium impurity removal from a rare earth element pregnant leach solution using magnesium carbonate. *Sci. Rep.* **2025**, *15*, 15951. [CrossRef] [PubMed]
30. Wu, D.; Xiao, X.; Guo, A.; Lan, Q.; Wang, H.; Ge, L.; Wen, X.; Sun, L.; Liao, C. Synchronized removal of non-rare earth ions (Al3+, Fe3+, Th4+, U6+, and F−) from rare earth leach solutions using lanthanum-cerium oxides for pH adjustment. *Hydrometallurgy* **2025**, *238*, 106572. [CrossRef]
31. Zhu, Y.; Li, J.; Xie, D.; Zhang, H.; Li, M.; Xu, B.; Zhang, X.; Xie, Y.; Qi, T. Aluminum Removal from Rare Earth Chloride Solution through Regulated Hydrolysis via Electrochemical Method. *Separations* **2024**, *11*, 149. [CrossRef]
32. Xie, D.; Li, J.; Zhang, H.; Zhu, Y.; Zhang, X.; Liu, K.; Xie, Y.; Qi, T.; Huang, Z. A novel electrochemical method for the removal of aluminum from ionic rare earth leachate. *Sep. Purif. Technol.* **2024**, *345*, 127296. [CrossRef]
33. Wang, C.; Li, J.; Xie, D.; Liu, X.; Zan, J.; Chang, L.; Lai, Y.; Xie, Y.; Zhang, X.; Zhang, H.; et al. Enhanced selectivity for the removal of Al^{3+} from the simulated rare earth leachate via a 3D electrochemical hydrolysis process. *Desalination* **2026**, *620*, 119679. [CrossRef]
34. Zeng, Z.; Gao, Y.; Liu, C.; Sun, X. A novel functionalized ionic liquid [DOC4mim][DEHG] for impurity removal of aluminum in rare earth leaching solution. *Sep. Purif. Technol.* **2022**, *296*, 121388. [CrossRef]
35. Zhang, N.; Li, F.; Xue, H.; Wang, Z.; Qiu, S.; Fan, B.; Cheng, Y.; Zhang, X. High-efficiency process of aluminum removal from rare earth solutions using a readily industrialized ionic liquid. *Hydrometallurgy* **2024**, *223*, 106224. [CrossRef]

36. Wang, J.; Xu, H.; Cao, Y.; Wu, Y.; Fan, G.; Fu, B.; Ma, L.; Kang, Y.; Sun, X.; Deng, J. Study on selective green leaching of rare earth elements from coal gangue using mechanochemical activation. *J. Environ. Chem. Eng.* **2024**, *12*, 114623. [CrossRef]
37. Hou, S.; Zhang, B.; Li, W.; Zhao, T.; Da, Z.; Liu, C. An Environmentally Friendly Sulfuric Acid Decomposition Strategy for Mixed Rare Earth Concentrate. *Minerals* **2024**, *14*, 185. [CrossRef]
38. Li, W.; Sun, J.; Zhang, X.; Cheng, S.; Ding, X. Influence of the screw-thread rod matrix on the magnetic capture behavior of bastnaesite. *Powder Technol.* **2024**, *440*, 119738. [CrossRef]
39. Ma, S.; Xu, H.; Chen, Y.; Xu, Y.; Gao, K.; Liu, X.; Hou, S.; Liu, L. Mineral phase transition and kinetics during the roasting of synthetic monazite with magnesium chloride hexahydrate. *Results Eng.* **2026**, *32*, 112177. [CrossRef]
40. Zhou, L.; Peng, T.; Sun, H.; Hui, T. Mechanism and kinetics of iron removal in Fe-Al-H_2SO_4 system by coordination precipitation. *Environ. Chem. Engin.* **2021**, *9*, 105241. [CrossRef]
41. Hamada, Y.Z.; Bayakly, N.; Peipho, A.; Carlson, B. Accueffciency potentiometric studies of chromium-citrate and ferric-citrate complexes in aqueous solutions at physiological and alkaline pH values. *Synth. React. Inorg. Metal.-Org. Nano-Met. Chem.* **2006**, *36*, 469–476. [CrossRef]
42. Kuan, W.H.; Wang, M.K.; Huang, P.M.; Wu, C.W.; Chang, C.M.; Wang, S.L. Effect of citric acid on aluminum hydrolytic speciation. *Water Res.* **2005**, *39*, 3457–3466. [CrossRef] [PubMed]
43. Ma, L.; Nie, Z.; Xi, X. Cobalt recovery from cobalt-bearing waste in sulphuric and citric acid systems. *Hydrometallurgy* **2013**, *136*, 1–7. [CrossRef]
44. Ma, C.; Zhu, X.; Li, W. Extraction and separation of vanadium (IV) by EHEHPA with citric acid complexing iron (III) from sulfate leaching solution. *Sep. Purif. Technol.* **2023**, *316*, 123720. [CrossRef]

Disclaimer/Publisher's Note: The statements, opinions and data contained in all publications are solely those of the individual author(s) and contributor(s) and not of MDPI and/or the editor(s). MDPI and/or the editor(s) disclaim responsibility for any injury to people or property resulting from any ideas, methods, instructions or products referred to in the content.